Biosystems Engineering (2007) **96** (2), 139–149
doi:10.1016/j.biosystemseng.2006.10.012
AE—Automation and Emerging Technologies

ELSEVIER

Development of an Autonomous Navigation System using a Two-dimensional Laser Scanner in an Orchard Application

Oscar C. Barawid Jr.; Akira Mizushima; Kazunobu Ishii; Noboru Noguchi

Bio-production Engineering, Graduate School of Agriculture, Hokkaido University, Kita 9, Nishi 9, Kita Ku, Sapporo 060-8589, Japan; e-mail of corresponding author: noguchi@bpe.agr.hokudai.ac.jp

(Received 4 February 2006; accepted in revised form 22 October 2006; published online 15 October 2006)

The objective of this study was to develop an automatic guidance system capable of navigating an autonomous vehicle travelling between tree rows in a real-time application. The study focused solely on straight line recognition of the tree rows using a laser scanner as a navigation sensor. A 52 kW agricultural tractor was used as the platform on which the laser scanner was mounted. A Hough transform was used as the algorithm to recognise the tree row. An auto-regression method eliminated the white Gaussian noise in the laser scanner data. A calibration method was used to select the offset position of the laser scanner and to correct the heading and lateral error evaluation. An appropriate speed for tractor was also determined. By obtaining an accuracy of 0·11 m lateral error and 1·5° heading error, it was possible to navigate the robot tractor autonomously between the orchard row crops.

1. Introduction

The application of autonomous navigation in an orchard is an ideal task because the same operations are repeatedly performed year after year. Usually in an orchard autonomous navigation, path planning is one of the most important tasks. An autonomous vehicle needs a path navigation to follow to perform its tasks. Most of the developed researches about path planning in orchards were map-based applications wherein the autonomous vehicle could only be used in a specific orchard site.

Applying autonomous navigation in a map-based application requires path planning before the vehicle can perform its tasks. Path planning basically refers to map generation where a thorough survey of the orchard is of the utmost priority. In a map-based application, the surveyed area is the only place where the tractor can travel. Another map needs to be provided for the next area and so on. This task of surveying and map generation will prove to be time consuming for the farmer or orchard owner. Commonly used navigation sensors include a real-time kinematic global positioning system (RTK-GPS), a laser radar, an inertial sensor unit, a laser scanner, a geomagnetic direction sensor, a posture sensor, and a charged coupled device (CCD) camera. Most of these studies of automatic guidance systems dealt with spatial positioning-sensing systems and steering control systems for following a predetermined path (Noguchi & Hideo, 1997; Noguchi *et al.*, 1997).

The hough transform based vision algorithm for crop row detection of an automated agricultural vehicle (Rovira-Más *et al.*, 2005) used vision-based method for detecting crop rows. This study is a similar application on which used Hough transform technique was also used in extracting navigation information from image data for grain crop rows tracking. A stereovision based crop row detection method for tractor automated guidance (Kise *et al.*, 2005) used a stereovision based agricultural machinery guidance system. The algorithm consists of functions of stereo-image processing, elevation map creation and navigation point determination for crop row detection. The research also dealt with the crop row detection for autonomous tractor guidance.

Notation

$\boldsymbol{A}_k$	theoretical autocorrelation function in k+1 series	T	effective series number
a, b	offset position of the laser scanner in local coordinate system, m	T	transform operator
$\boldsymbol{a}_p$	auto-regression parameters/parameter coefficients	x	coordinate
c	Y intercept of the line	$x(j)$	theoretical autocorrelation value in Yule–-Walker equation
D	distance from the GPS antenna to the perpendicular wall, m	x_t	served series data with respect to time (t), m
d, d_i	measured distance between obstacle and the laser scanner, m	y	coordinate
E	distance from laser scanner centre point to the perpendicular wall, m	α, β	straight line coefficient of the perpendicular wall
E_s, N_s	transform position of the perpendicular wall to universal transverse Mercator (UTM) coordinates, m	δ	offset angle of the laser scanner position, deg
F	difference of distances D and E, m	ε_i	minimum error
$F_{pe(k)}$	final prediction error in terms of the kth model order, m	ε_l	lateral error offset of the vehicle, m
k	estimated number of model order	ε_t	an white noise or the error function, m
m	slope of the line	η	angle between the vehicle local coordinates and the UTM coordinates, deg
n	number of observed data	θ	orientation angle with respect to the X axis, deg
$\boldsymbol{R}_k$	sample auto-covariance function in k+1 series	ϕ_i	relative angle acquired by the laser scanner, deg
r	shortest distance from the origin to the line, m	κ	angle between the laser scanner and the perpendicular wall, deg
r_i	distance between laser scanner and orchard row, m	v	angle of the perpendicular wall with respect to UTM coordinates, deg
r_L	distance to left side of the laser scanner computed in a Hough transform, cm	ρ	transformation angle, deg
r_R	distance to right side of the laser scanner computed in a Hough transform, cm	$\sigma_{\hat{\varepsilon}}^2$	maximum likelihood estimate of the residual variance
		θ	deflection angle between orchard row and vehicle direction, deg
		ψ	angle between the perpendicular wall and the vehicle local coordinate system, deg

The concept behind this research is to develop an autonomous navigation system that will work in any given orchard without having to rely on a planned path. An autonomous navigation system in a real-time application has many uses such as orchard design, water management, robot tractors, weed management, canopy management, remote sensing, mechanical harvest, and many more depending on its application. Aside from the obvious advantage of being time-saving because the task of pre-surveying is already omitted, this form of autonomous navigation can be used on occasions when a GPS becomes non-functional as is the case when there are obstructions in the environment. A global sensing method works only in open spaces (Hakura & Yoshikazu, 2001).

This research used a two-dimensional (2D) laser scanner as the navigation sensor to explore the surrounding environment. An agricultural tractor was modified into a robot tractor to track the navigated path in an orchard and a laser scanner detected the navigation information necessary for guiding the tractor, such as lateral error and heading error.

The four methods applied in this research were a tree row detection algorithm method, a laser scanner calibration method, a noise removal method using auto-regression (AR), and a method for the determination of the appropriate speed of the robot tractor that has the minimum guidance error. The tree row detection algorithm extracted straight lines from the orchard tree row image. Auto-regression eliminated the Gaussian noise present in lateral error and heading error. The calibration method determined the equipped position and angle of the laser scanner. Finally, an appropriate speed for autonomous navigation was determined by conducting different autonomous field runs at various speeds.

2. Research components

This research used a 56 kW agricultural tractor, which was modified into a robot tractor. The robot tractor controlled steering, transmission (forward, neutral, and backward), power take-off (PTO), engine speed, brake system, and three-point hitches (up and down). The navigation sensor was a 2D laser scanner (LMS 219, Sick AG, Division Auto Indent, Germany), which was mounted on the front of the robot tractor. The laser scanner can detect the maximum distance and angle of the surrounding environment of 80 m and 180°, respectively. The laser range has two adjustable modes of 8 and 80 m and has an average error of 35 mm and 5 cm, respectively. The angle resolution has three adjustable modes of 0·25°, 0·5°, and 1° and has a response time of 53, 26, and 13 ms, respectively. In this research, the distance range of the laser scanner was set to 80 m mode. The angle range was set to 1° mode and response time was set to 13 ms mode. The distance error of the laser scanner is ±5 cm. For the calibration of the laser scanner mounted on the front of the robot tractor, RTK-GPS was used as the positioning sensor with an accuracy of ±2 cm, and a fibre optic gyroscope (FOG) was used as the heading sensor with a heading accuracy of ±0·05°/h. A wall was used as the reference line for the calibration perpendicular to the GPS antenna and laser scanner centre point, and was named as the perpendicular wall. A total station, which is a transit surveying instrument (APL-1A, TOPCON Ltd., Japan), was used to get the relative position of the perpendicular wall (X, Y, and Z axes) with an accuracy of ±3 mm for fine mode and ±10 mm for course mode. The total station was set to fine mode setting. The RTK-GPS and FOG were connected to a laptop personal computer (PC) with an RS-232 cable. *Figure 1* shows the schematic diagram of the robot tractor and its research components.

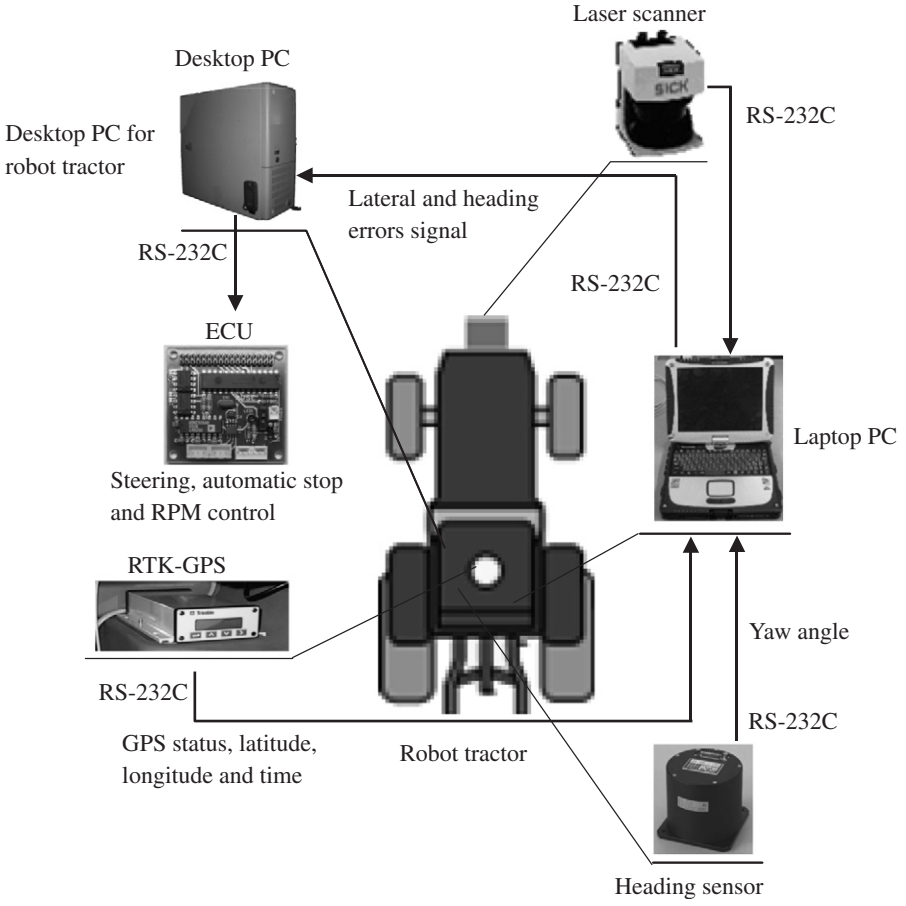

Fig. 1. Schematic diagram of the robot tractor and its research components; PC, personal computer; RTK-GPS, real-time kinematic global positioning system; ECU, electronic control unit; RS 232C, recommended standard 232 connector

3. Methods

3.1. *Orchard rows detection algorithm*

3.1.1. *Hough transform sampling*

The Hough transform used in this research as an orchard row detection algorithm was patented by Paul V.C. Hough in 1962. It is used for linear or circular detection. The main advantage of using a Hough transform, compared to an alternative commonly used method such as least-squared error method of fitting lines to image data, is that even if group points vary to some extent, seeking for a straight line is still possible. Also, processing is collectively possible even when there are two or more straight lines in the image data. The point that has the majority of intersections serves as the line equation. On the contrary, the disadvantage is that in order to plot curves (*i.e.* sinusoids) for every observation point (x_i, y_i) in Cartesian image space to r–θ polar Hough parameter space, the load of computational complexity is large.

Consider the normal Cartesian equation of a straight line, which is generally on an XY plane:

$$y = mx + c \tag{1}$$

where: m is the slope and c is the Y intercept. Consider some points of the image data where a straight line can be obtained from its edge. Transform the points into r–θ normal representation of a line in Hough space (only points where the line pass through) as shown in *Fig. 2(a)*. The shortest distance from the origin can be obtained equivalent to Eqn (2) (Gonzales & Wood, 1993).

$$r = x\cos\theta + y\sin\theta \tag{2}$$

In Eqn (2), the line is defined in terms of r and θ, where r is the shortest distance from the origin to the line and θ is the orientation angle with respect to the X axis. For any point (x, y) on this line, r and θ are constant. Equation (2) can be considered a relation between the coordinates (x, y) of some points in the edge image and the value of the parameters (r–θ), which defines the equation of the line. The points in Cartesian space correspond to a sine wave r–θ polar in Hough parameter space shown in *Fig. 2(b)*. In *Fig. 2(b)*, the point where the majority of these sinusoids intersect serve as the equation of the line. For example, the value of distance r is equivalent to 6·06 units and the angle θ is equivalent to 40°. The line of the equation is $y = -1{\cdot}19x + 9{\cdot}4$.

3.1.2. *Orchard rows recognition using a laser scanner*

The Hough transform extracted a straight line in an orchard row from the data obtained by the laser scanner in a real-time circumference environment. The purpose

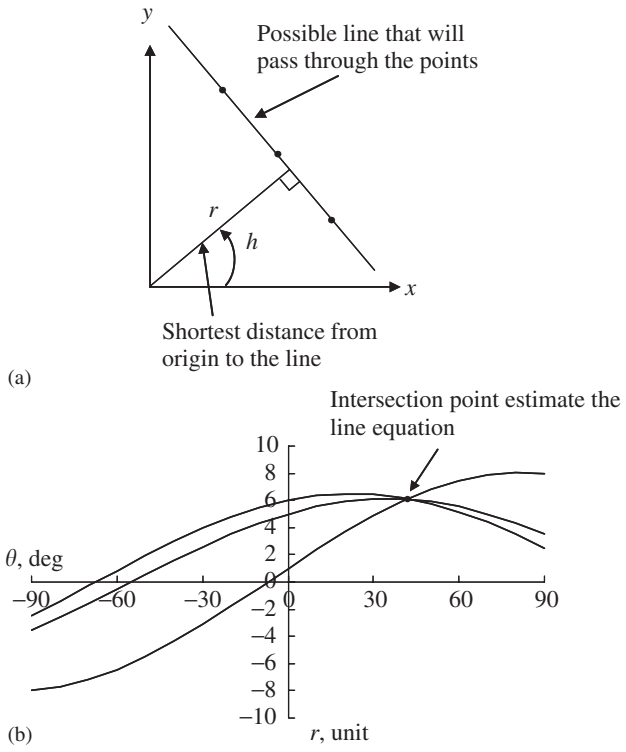

Fig. 2. The Hough transform in r–θ space: (a) r–θ space normal representation of a line in Hough transform; (b) points transform to sinusoids in r–θ space; r, shortest distance from the origin of the line; θ, orientation angle

of the Hough transform algorithm is to automatically detect the orchard tree lines and to provide lateral offset and heading measurements, which can be sent to a vehicle controller as the target course. The laser scanner was attached on the front of the robot tractor and positioned 70 cm above the ground as shown in *Fig. 3*. This laser scanner detects distance d and angle θ in real time about the circumference environment. *Figure 4* shows the outline of the orchard row recognition using the laser scanner. In the figure, the points were the components of the orchard trees scanned by the laser scanner. Using r–θ parameterisation space, a point in Cartesian space (x_i, y_i) corresponds in the r–θ space, Eqn (2) can be written in the form of Eqn (3):

$$r_i = d_i\cos(\phi_j - \theta) \qquad (0 \leqslant i \leqslant 180, \quad 0 \leqslant \theta \leqslant 180) \tag{3}$$

In Eqn (3), r_i is the shortest distance between the laser scanner and the orchard row, d_i is the measured distance between the obstacle and the laser scanner, ϕ_i is the relative angle of the obstacle with respect to the laser scanner detection, and θ is the deflection angle between the orchard row and the laser scanner. The main advantage of the r–θ space is that quantisation is relatively easy because not all of the parameter space

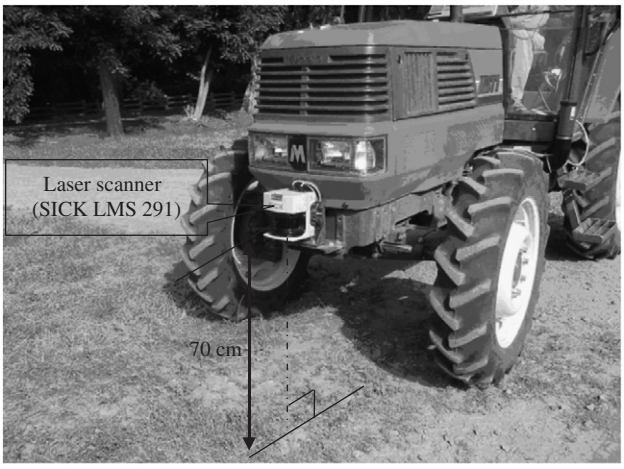

Fig. 3. Attachment position of the laser scanner in front of the robot tractor

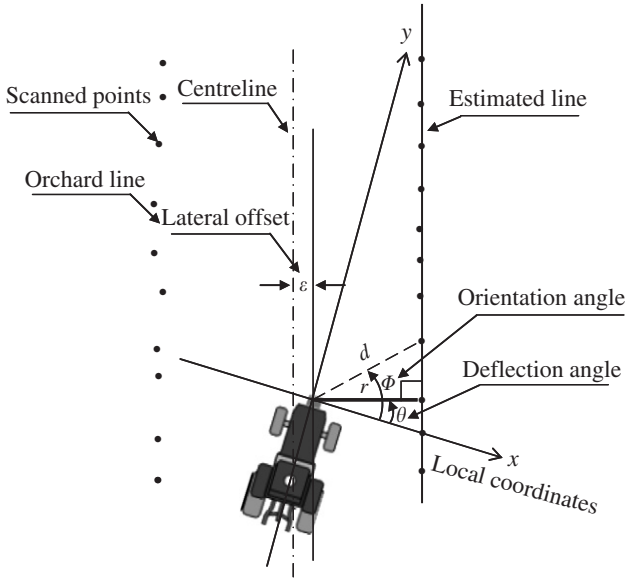

Fig. 4. An outline on how to recognise the orchard rows using Hough transform as algorithm; r, shortest distance perpendicular to the estimated line; d, distance between the obstacle and the laser scanner; ϕ, orientation angle with respect to X axis; ε, lateral offset; θ deflection angle

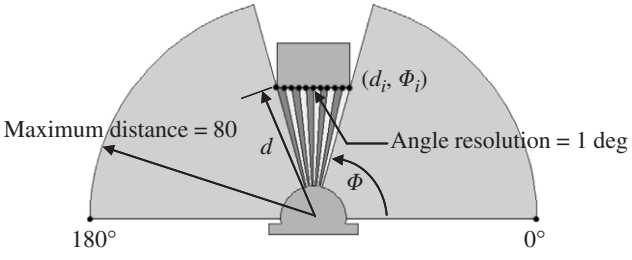

Fig. 5. Laser scanner diagram with angle range set to 180°, distance range was set to 80 m, and the direction of transmission was counterclockwise; d, distance between obstacle and the laser scanner; ϕ, orientation angle with respect to X axis

needs to be considered. Looking at *Fig. 3(b)*, all the sinusoids have the same period, and therefore θ_i can be limited to any angle range depending on the application without losing its generality. In this research, the θ_i limit was $0 \leqslant i \leqslant 180$ and ϕ_j limit was $0 \leqslant j \leqslant 180$. *Figure 5* shows the laser scanner diagram with set angle and distance range.

Lateral error ε_l can be calculated using Eqn (4). Using the data obtained by the laser scanner, lateral offset can be evaluated and become the target run course of the robot tractor.

$$\varepsilon_l = \frac{r_L - r_R}{2} \tag{4}$$

In this equation, the solution was made to both positive value and negative value. In positive case, the distance to the right-hand side is denoted by r_R in cm and the distance to left-hand side is denoted by r_L in cm with respect to the main target course. The actual captured points of the laser scanner were shown in *Fig. 6*, where the black points correspond to the components of the trees. Using the Hough transform, the laser scanner could recognise the orchard rows as straight lines as shown in *Fig. 6*, where the straight lines were plotted in the orchard rows. The black line in the middle of the orchard was recognised as the main target course of the robot tractor. It served as the lateral offset for the robot tractor navigation to follow. In plotting these captured points into sine wave r–θ space shown in *Fig. 7*, a cluster of intersections of sinusoids can be seen. The majority of intersection of these sinusoids which estimated the equation of the line would become the orchard row lines. These points of majority intersections served as the solution for recognising the orchard rows.

3.2. *Calibration method of the mounted sensor*

Calibrating the laser scanner was an important task to be done in order to know whether it was properly aligned with respect to the reference coordinates. The reference coordinates pertain to the robot tractor coordinate axes. It is necessary to evaluate the exact attachment position of the laser scanner because it will affect the accuracy evaluation of the robot tractor such as the lateral error and heading error. For sensors such as a video camera, a laser range finder, an ultrasonic sensor, a 2D laser scanner and a GPS (global positioning system), *etc*., the position and orientation of the sensor affects the geometric interpretation of its measurements (Pless & Zhang, 2003). The purpose of calibrating the laser scanner is to get the offset values. An outline for the calibration of the laser scanner using perpendicular wall was shown in *Fig. 8*. The offset was between the RTK-GPS antenna and the laser scanner

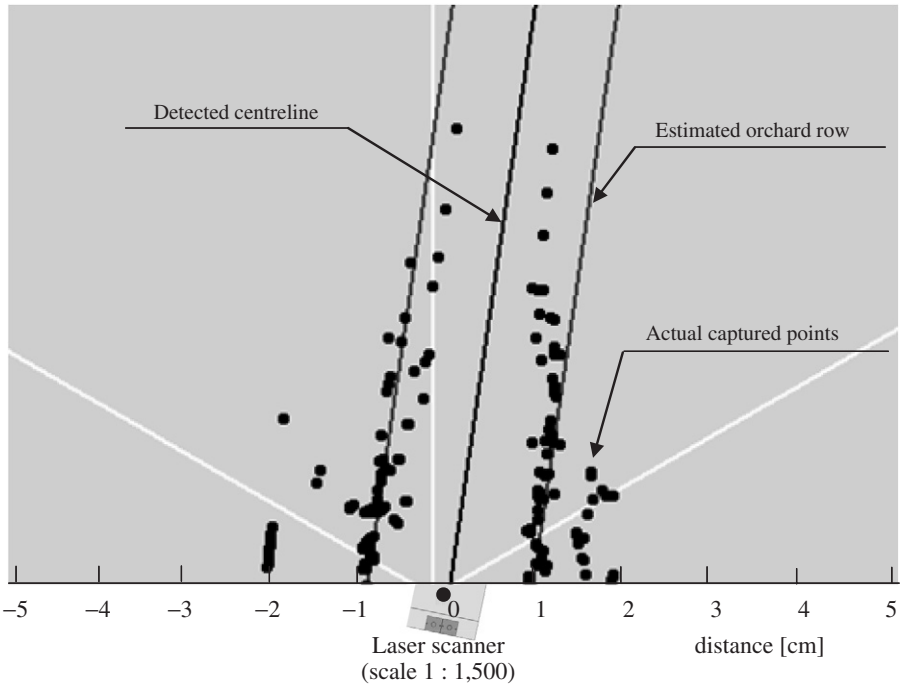

Fig. 6. Actual captured points by the laser scanner in a computer window of the orchard tree rows

centre point. In order to evaluate the relative position of the laser scanner correctly, a calibration test was performed using a perpendicular wall. The perpendicular wall relative position (X, Y and Z axes) was measured by the total station, and then the edge points absolute position were measured by the RTK-GPS. Transforming the local coordinate system (x, y) was obtained by the total station into universal transverse Mercator (UTM) coordinate system (E_s, N_s) by using the Eqn (5).

$$\begin{pmatrix} E_s \\ N_s \end{pmatrix} = \begin{pmatrix} \cos\ \rho & -\sin\ \rho \\ \sin\ \rho & \cos\ \rho \end{pmatrix} \begin{pmatrix} x_s \\ y_s \end{pmatrix} + \begin{pmatrix} E_0 \\ N_0 \end{pmatrix} \quad (5)$$

where: the angle ρ is the transformation angle in deg, (E_0, N_0) is the starting point of the perpendicular wall in UTM coordinates in m at the northen direction. The next parameter to be explained in *Fig. 8* is the offset values between centre point of the laser scanner and the GPS antenna. The symbols a and b denote the laser scanner offset in m at the vehicle coordinate system, and δ is the offset angle of the laser scanner in degrees at the vehicle coordinate system. Solving for the distance E of the laser scanner and the wall can be computed from Eqn (3). To solve the distance D between perpendicular wall and GPS antenna, the straight line equation of the perpendicular wall is needed to use Eqn (6):

$$\alpha x + \beta y + c = 0 \quad (6)$$

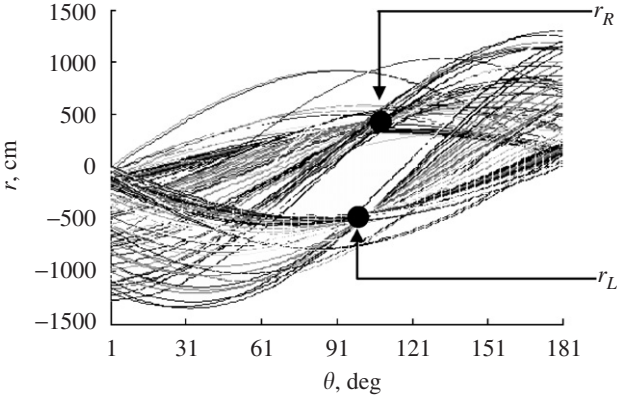

Fig. 7. Illustration of the captured points of the laser scanner transform to sinusoids in r–θ space; r_R, distance to right side of the laser scanner computed in Hough transform; r_L, distance to left side of the laser scanner computed in Hough transform

where α and β are coefficients. Using the perpendicular distance relation between the perpendicular wall and GPS antenna, the distance D can be solved by Eqn (7):

$$D = \frac{\text{abs}|\alpha x + \beta y + c|}{\sqrt{\alpha^2 + \beta^2}} \quad (7)$$

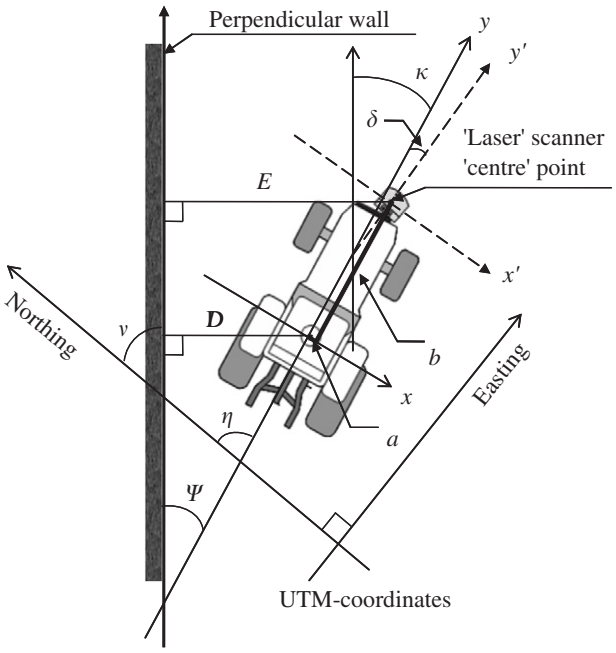

Fig. 8. Calibration method outline using a perpendicular wall as the reference line for getting the laser scanner exact position; a and b, offset position of the laser scanner in local coordinate system; δ, offset angle of the laser scanner position; ψ, angle between the perpendicular wall and vehicle coordinate system; η, angle between the vehicle local coordinates and the universal transverse Mercator (UTM) coordinates; D, distance from GPS antenna to the perpendicular wall; E, distance from the laser scanner centre point to the perpendicular wall; x–y, robot tractor coordinate; x′–y′, laser scanner coordinate

The angle ψ between the perpendicular wall and vehicle coordinate system is given by

$$\psi = \eta - v \tag{8}$$

where: η is the angle of the vehicle direction in deg with respect to the UTM coordinate; and v is the angle of the perpendicular wall in deg with respect to the UTM coordinate. The equation for solving the offset angle δ of the laser scanner is shown in Eqn (9).

$$\delta = \kappa - \psi \tag{9}$$

Using the Hough transform, κ is the angle in deg between the exact position of the laser scanner and the perpendicular wall, computed from the data obtained by the laser scanner during the autonomous navigation. The centre point of the laser scanner from the perpendicular wall is denoted by E in m. The value of E can be computed from the data obtained by the laser scanner for distance d and angle θ using the Hough transform. The distance from the GPS antenna to the perpendicular wall is denoted by D in m. Since it exists on the straight line, the position of the laser scanner can be calculated using Eqn (10) in vehicle coordinate system.

$$a\cos\psi + b\sin\psi = E - D \tag{10}$$

However, E–D values have measurement errors. Through using the least–squares method, the minimum errors were obtained. The error of measurement i was acquired in a straight line for n observations as

$$a\cos\psi_i + b\sin\psi_i + D_i - E_i = 0 \tag{11}$$

Assigning the F_i as

$$F_i = D_i - E_i \tag{12}$$

Using least-squared method (LSM), the minimum error (ε_i) can be calculated in Eqn (13):

$$\varepsilon_i^2 = \left(a\cos\psi_i + b\sin\psi_i + F_i\right)^2 \tag{13}$$

Solving for the least-squares estimates S_ε by summing of all observation data:

$$S_\varepsilon = \sum_{i=0}^{n} \varepsilon_i^2 \tag{14}$$

Using partial derivatives, the minimum error can be calculated in Eqns (15) and (16) which are set to 0:

$$\frac{\partial S_\varepsilon}{\partial a} = \sum_{i=0}^{n}(2a\cos^2\psi_i + 2b\ \cos\psi_i\sin\psi_i + 2\cos\psi_i F_i) = 0 \tag{15}$$

$$\frac{\partial S_\varepsilon}{\partial b} = \sum_{i=0}^{n}(2a\ \cos\psi_i\sin\psi_i + 2b\sin^2\psi_i + 2\sin\psi_i F_i) = 0 \tag{16}$$

The values of the offset position of the laser scanner were $a = -0{\cdot}056$ m, $b = 2{\cdot}57$ m and $\delta = 2{\cdot}8^\circ$ from the vehicle coordinates.

3.3. *Noise removal and time series analysis using an auto-regression method*

3.3.1. *Estimation of auto-regressive coefficients*

The results obtained in the Hough transform have a noise data. The noise data is contained in the lateral offset and heading error. This noise will cause the lateral offset and heading error to make the steering controller unstable. In order to get the minimum error in lateral and heading error, a noise removal method using linear time series general AR was used to refine the output data which does not have a time delay. Defining the general auto-regressive model of order k, denoted as AR(k) (Kendall & Ord, 1990)

$$\varepsilon_t = x_t + a_1 x_{t-1} + \cdots + a_k x_{t-k}, \qquad t = k+1, \ldots, n, \tag{17}$$

where $a_1, \ldots, a_k$ are the auto-regressive coefficients and $x_1, \ldots, x_n$ are an observed series of data. However, although there are n observations, because x_{t-k} are used to model x_t the effective series length is

$$T = n - k \tag{18}$$

where: k is the order of model; T is the reduced number of observations; n is the number of observations; and ε_t is the Gaussian white noise/error. Assume the $E(\varepsilon_t) = 0$, being normal variables with zero mean and $\text{var}(\varepsilon_t) = E(\varepsilon_t^2) = \sigma_\varepsilon^2$, unit variance, without the loss of generality.

The problem in AR analysis (Bourke, 1998) is to derive the best values for $a_1, \ldots, a_k$ or the auto-regressive coefficients given a series x_t. The majority of methods assume the series x_t is linear and stationary. The case of conditional maximum likelihood estimates of the parameters (Priestley, 1981) is identical with the least square estimates. Thus, solving for the values of auto-regressive coefficients $(a_1, \ldots, a_k)$ in matrix form

$$\boldsymbol{a}_p = \boldsymbol{R}_k^{-1} - 1\boldsymbol{A}_k \tag{19}$$

where

$$\boldsymbol{a}_p = [a_1, a_2, \ldots, ak]^{\mathrm{T}}, \quad \boldsymbol{A}_k = [-A(1), -A(2), \ldots - A(k)]^{\mathrm{T}} \tag{20}$$

and

$$\boldsymbol{R}_k = \begin{bmatrix} R(0) & R(1) & R(k-1) \\ R(1) & R(0) & R(k-2) \\ \cdot & \cdot & \cdot \\ \cdot & \cdot & \cdot \\ R(k-1) & R(k-2) & R(0) \end{bmatrix} \tag{21}$$

The approximate expressions (Priestley, 1981) for the maximum likelihood (or least squares) estimates $a_1, \ldots, a_k$ may be obtained by computing the first $(k+1)$ sample auto-covariances $R(0)$, $R(1), \ldots, R(\mathrm{k})$ and then solving the set of linear equations using the Yule–Walker equations which express the theoretical values of the auto-regressive coefficients $(a_1, \ldots, a_k)$ in terms of the theoretical auto-covariance $x(j)$ function.

$$x(j) = a_1 x(j-1) + \cdots + a_k x(j-k), \qquad j = 1, \ldots, k. \tag{22}$$

3.3.2. *Determining the order of the model*

There is no straightforward way to determine the correct model order. An order just after the point at which the root-mean-square (RMS) error flattens out is usually an appropriate order (Bourke, 1998). But there is a formal technique for AR model order determination. The more refined version of a residual variance plot is the Akaike's final prediction error $F_{pe(k)}$

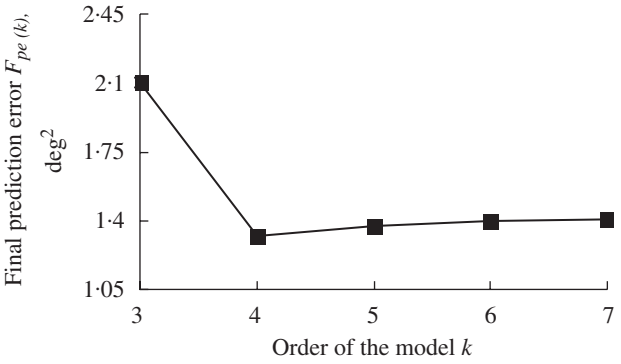

Fig. 9. Final prediction error $F_{pe(k)}$ as a function of the maximum likelihood estimate of the residual variance

(McQuarrie & Tsai, 1998). This method starts by fitting AR models of increasing order k, and for each k one computes, the expression:

$$F_{pe(k)} = \frac{n+k}{n-k}\sigma_\varepsilon^2 \tag{23}$$

where: n is the number of observations to which the model is fitted, and σ_ε^2 is the maximum likelihood estimate of the residual variance, can be solved in Eqn (24).

$$\sigma_\varepsilon^2 = R(0) + a_1 R(1) + \cdots + a_k R(k) \tag{24}$$

Plotting $F_{pe(k)}$ values against k, which was shown in *Fig. 9*, shows the value of the final prediction error for increasing numbers of order of the model k. The graph will, in general, show the definite minimum at a particular value of k, and the basis of Akaike's method is to use that value of k at which the final prediction error $F_{pe(k)}$ attains its minimum as the appropriate order of the model. The value of k that obtained the minimum value was four as the appropriate order of the model or auto-regression (AR4).

3.4. *Determination of the appropriate speed of the robot tractor*

Determination of the appropriate speed is one of the important tasks to do in the real-time application of an autonomous vehicle. The aim of determining the appropriate speed of the robot tractor is to get the minimum guidance error. The tractor speed in autonomous navigation will affect the accuracy of the robot tractor performance such as increase in heading and lateral error. To get the appropriate speed of the robot tractor, different autonomous field runs were conducted at various speeds. Six different runs were conducted at 0·36, 0·48, 0·62, 0·86, 1·23 and 1·43 m/s. The robot tractor steering input frequency was set to 10 Hz and the

data output frequency was set to 10 Hz. The appropriate speed for the autonomous navigation was determined as 0·36 m/s. The 0·36 m/s speed was the basis for evaluating this entire research.

4. Results and discussion

4.1. *Evaluating the accuracy of the autonomous run*

The developed automatic navigation system was tested in the Hokkaido University, Sapporo, Japan. The selected test site was approximately 40 m by 3 m in length and width. The area, which resembled an orchard, was spanned with trees in two vertical rows. Since the test area was not an actual orchard, there were some parts in the experiment site where trees were sparse. Hence, irregularities in the form of gaps between trees were given due consideration in the study. Different test runs (0·36, 0·48, 0·62, 0·86, 1·23 and 1·43 m/s) were made throughout the whole expanse of the area notwithstanding the presence of some gaps between the trees. A single course run was the run throughout the whole expanse of the tree rows. The single course run was referred to as the complete run. The data obtained from this test run was then consequently evaluated. In order to get the most accurate data, a specified portion in the experiment site where there were no apparent breaks between trees were taken and considered as the basis for evaluating the autonomous accuracy of the robot tractor. The test runs conducted on the area that best resembled an orchard due to the uniformity and alignment of trees was called the specified run. The robot tractor can navigate autonomously between the tree rows even in the presence of some spaces between trees.

The attachment position of the laser scanner was determined using the calibration method as $a = -0{\cdot}056$ m, $b = 2{\cdot}57$ m and $\delta = 2{\cdot}8^\circ$ from the vehicle coordinates. The positioned data obtained by this method served as the offset values for evaluating the accuracy in the autonomous run of the robot tractor. Before applying the AR analysis to the raw data obtained by the laser scanner, the actual data should be calculated first using the offset values of the laser scanner. The actual data was the result of the difference between the raw data and the offset values. The actual data for lateral and heading errors were 0·21 m and 2·7 °, respectively, in 0·36 m/s run.

A calculation was made by applying AR analysis to the actual data to get the minimum output in terms of heading and lateral mean error. The correct model order was also determined using Akaike's method for solving the final prediction error $F_{pe(k)}$. *Figure 10* shows the

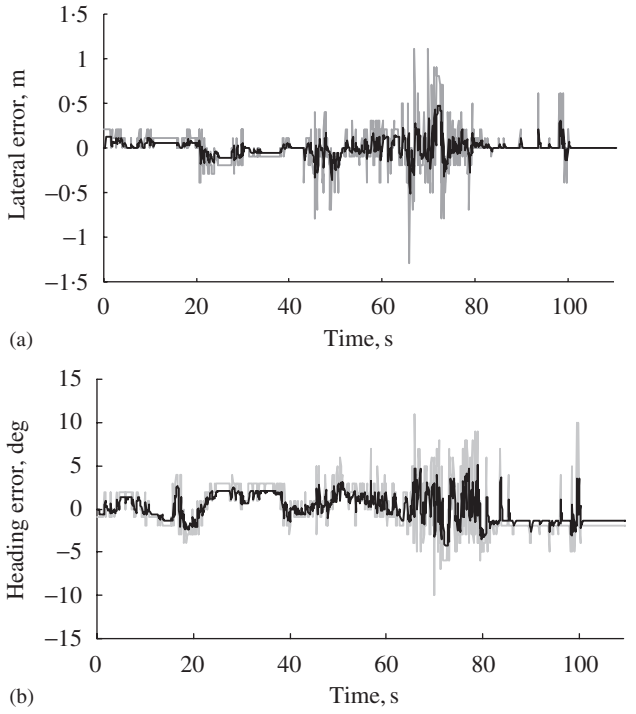

Fig. 10. Comparison of raw data and auto-regression, (AR4) estimated error: (a) comparison of raw data error and auto-regression, (AR4) estimated error in heading error obtained by the laser scanner; (b) comparison of raw data error and auto-regression, AR (4) estimated error in lateral error obtained by the laser scanner; ——, raw data error; ——, AR(4) estimated error

comparison of the actual data and the AR4 estimated error in heading and lateral mean errors. In the figures, the Gaussian noise was eliminated using the AR analysis with a correct model order of four or AR4. The grey projections corresponded to the actual data for estimated errors both in lateral and heading errors with the Gaussian noise included, while the black projections corresponded to the estimated output data both in lateral and heading errors applying the AR4. The root mean squares (RMS) of heading and lateral errors applying the AR4 to a complete run were 0·19 m and 2·2 °, respectively. And the RMS of heading and lateral errors applying AR4 to a specified run were 0·11 m and 1·5 °, respectively. *Figure 11* shows the graphic representation of the evaluated autonomous accuracy. In the figure, the highest RMS lateral and heading errors in a specified run were 0·48 m and 7 °, respectively. These accuracy results were minimal in autonomous navigation and it has a uniform fluctuation accuracy error. This means that the steering has a stable condition in a specified run.

To ensure if the evaluated autonomous accuracy was enough for the autonomous navigation, a comparison of the stationary data and moving data was made as shown

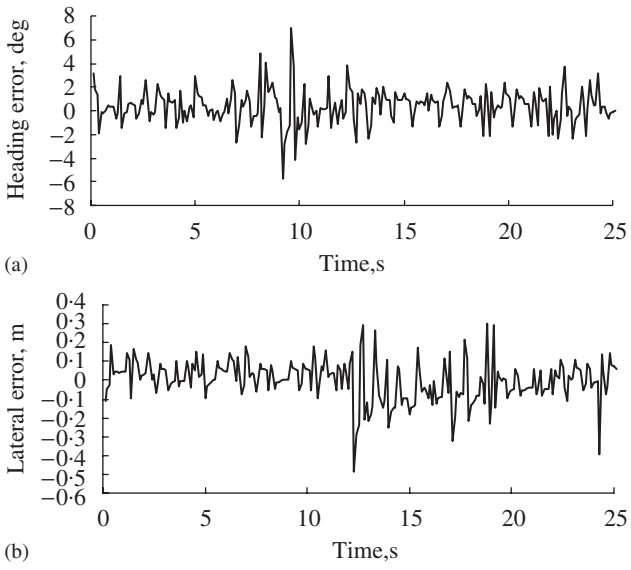

Fig. 11. Evaluated autonomous accuracy: (a) heading error of the autonomous run with a root mean square (RMS) error of 1·5°; (b) lateral error of the autonomous run with a root mean square (RMS) error of 0·11 m

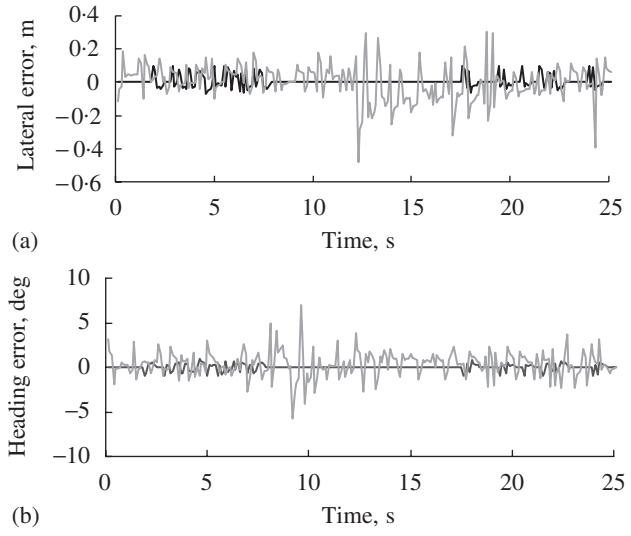

Fig. 12. Comparison of root mean square error between stationary data and moving data: (a) comparison of root mean square error between stationary data with mean error of 0·5° and moving data with mean error of 1·5° in heading error, (b) comparison of root mean square error between stationary data with mean error of 0·05 m and moving data with mean error of 0·11 m in lateral error; ——, moving data error; ——, stationary data error

in *Fig. 12*. In the figures, the grey projections correspond to the moving data of the evaluated autonomous accuracy, while the black projections represent the stationary data with a heading and a lateral mean error of 0·5° and 0·05 m, respectively. The evaluated autonomous accuracy of the robot tractor did not show significant deviation from the stationary data. Hence, it can be concluded that the lateral and heading mean error results were enough for navigating in an orchard real-time application.

4.2. *Evaluating the accuracy in various speeds*

Autonomous runs at various speeds were conducted and evaluated to know the most appropriate speed needed in this research. The run which yielded the least guidance error was considered the most appropriate speed. Each run calculated the lateral and heading mean errors from actual data to the AR4 application. Tables 1 and 2 showed the summary of the heading and lateral mean error of actual data and AR4 in complete run and specified run with respect to the various speed runs. The complete run evaluation was also included in the tables to show that the presence of gaps between the trees was irrelevant to the proper functioning of the autonomous robot tractor. In the tables, 0·36 m/s run have the minimum lateral and mean error. This speed was enough and appropriate to navigate the robot tractor between the orchard rows because the the resulting

Table 1
Summary of the root-mean-square (RMS) errors of lateral errors at different speeds of the robot tractor using data obtained from the laser scanner

Speed, m/s	*Actual data, m*	*Auto-regression (AR4), m*	
		Complete run	*Specified run*
0·36	0·21	0·19	0·11
0·48	0·73	0·44	0·14
0·62	0·56	0·49	0·19
0·86	1·32	0·76	0·36
1·23	0·48	0·22	0·21
1·43	1·12	0·83	0·36

Table 2
Summary of root-mean-square (RMS) errors of the heading errors at different speeds of the robot tractor using data obtained from the laser scanner

Speed, m/s	*Actual data, deg*	*Auto-regression (AR4), deg*	
		Complete run	*Specified run*
0·36	2·7	2·2	1·5
0·48	11·0	6·1	3·3
0·62	7·8	6·0	3·4
0·86	7·4	5·7	3·3
1·23	8·2	5·7	5·3
1·43	12·5	9·2	4·9

errors were relatively small, and it was the speed used in the evaluation of the autonomous accuracy of this research.

Other speed such as 0·48 m/s can also be used to evaluate the autonomous accuracy in this study because the mean errors were also minimal. But the researcher preferred to use the 0·36 m/s in this research due to its very minimal error both in lateral and heading errors.

5. Conclusion

This research developed an autonomous navigation system suitable for real-time applications such as orchard navigation without using a global positioning system. A two-dimensional laser scanner was used as the primary navigation sensor to detect the orchard rows. A calibration method determined the relative position of the laser scanner and served as the offset values to improve the accuracy of the autonomous navigation by correcting the lateral and heading mean error outputs. The auto-regression (AR) method was used to eliminate Gaussian noise and to obtain the minimum lateral and heading mean error. A total station measured the relative position of the perpendicular wall that was used to support the calibration process. Fibre optic gyroscope measured the heading angle. Conditional maximum likelihood estimates calculated the AR coefficients that were necessary for getting the estimated minimum mean error in AR analysis. An Akaike's final prediction error obtained the correct model order for getting the estimated minimum mean error in the AR analysis. As a result, the evaluated autonomous accuracy was 0·11 m and 1·5 ° in the lateral and in the heading mean error, respectively. To ensure that the evaluated accuracy was adequate enough for the autonomous navigation, a comparison of the stationary and moving data mean error was made. The stationary data or normal Gaussian noise has a heading and lateral mean error of 0·5 ° and 0·05 m, respectively. The results in moving data mean error was sufficient for autonomous navigation in a real-time application.

In this research, the appropriate speed was determined as 0·36 m/s based on the different runs with different speeds. This speed has the minimum mean error compared to these for other test runs.

References

Bourke P (1998). Auto-regression Analysis (AR). http://local.wasp.uwa.edu.au/pbourke/other/ar/ (August 11, 2006)

Gonzales R C; Woods R E (1993). Digital Image Processing. Addison-Wesley Publishing, USA

Hakura J; Yoshikazu A (2001). Self-localization based on ego motion detection using optic flow. Proceedings of the Fourth International Federation of Automatic Control Symposium on Intelligent Autonomous Vehicle, pp 320–331, Japan

Kendall S.M; Ord JK (1990). Time Series. British Library Cataloging in Publication Data. Great Britain.

Kise M; Zhang Q; Rovira Mas F (2005). A stereovision-based crop row detection method for tractor-automated guidance. Biosystems Engineering, **90**(4), 357–367 doi:10.1016/j.biosystemseng.2004.12.008

McQuarrie A; Tsai C L (1998). Regression and Time Series Model Selection. World Scientific, Singapore

Noguchi N; Hideo T (1997). Path planning of an agricultural mobile robot by neutral network and genetic algorithm. Biosystems Engineering, **18,** 187–204

Noguchi N; Ishii K; Terao H (1997). Development of an agricultural mobile robot using a geomagnetic direction sensor and image sensors. Journal of Agricultural Engineering, **67,** 1–15

Pless P; Zhang Q (2003). Extrinsic auto-calibration of a camera and laser range finder. Department of Computer Science and Engineering, Washington University, St. Louis

Priestley M B (1981). Spectral Analysis and Time Series, Vols. 1 and 2. Academic Press, New York

Rovira-Más F; Zhang Q; Reid J F; Will J D (2005). Hough-transform-based vision algorithm for crop row detection of an automated agricultural vehicle. Journal of Automobile Engineering, **219**(8), 999–1010